Glycomic profiling of invasive and non-invasive breast cancer cells

John A. Goetz · Yehia Mechref · Pilsoo Kang · Meei-Huey Jeng · Milos V. Novotny

Abstract Quantitative profiling of glycans with different structures appears essential for a better understanding of the cellular adhesion phenomena associated with malignant transformation and the underlying aberrant glycosylation of cancer cells. Using the recently developed glycomic techniques and mass-spectrometric measurements, we compare the N-linked and O-linked oligosaccharide profiles for different breast cancer cell lines with those of normal epithelial cells. Statistically significant differences in certain neutral, sialylated and fucosylated structures are readily discerned through quantitative measurements, indicating a potential of distinguishing invasive and non-invasive cancer attributes. The glycomic profile data cluster accordingly using Principal Component Analysis, verifying further glycobiological differences due to the differences between normal and cancer cell lines.

Keywords Glycomics · Invasive and non-invasive breast cancer cells · MALDI MS · Permethylation

J. A. Goetz · Y. Mechref (✉) · P. Kang · M. V. Novotny (✉)
Department of Chemistry, Indiana University,
800 E. Kirkwood Ave.,
Bloomington, IN 47405, USA
e-mail: ymechref@indiana.edu
e-mail: novotny@indiana.edu

J. A. Goetz · Y. Mechref · M.-H. Jeng · M. V. Novotny
National Center for Glycomics and Glycoproteomics,
Indiana University,
Bloomington, IN 47405, USA

M.-H. Jeng
Department of Medicine, Indiana University,
Indianapolis, IN 46202, USA

Introduction

The metastatic potential of cancerous cells is now widely attributed to their adhesive properties toward various blood-borne cells that feature receptors for different carbohydrate structures [1, 2]. The adhesion process is enhanced by certain aberrant glycosylated structures, which are different from those encountered on the surface of normal cells [3, 4]. While the general process governing the release of cells from the primary tumor to secondary sites has been extensively studied [5], relatively little is still known about the role of glycosylation and specific glycan structures (incorporated within the surface glycoproteins) during metastasis.

Whereas a growing body of knowledge on the glycosylation of cancer cells has come from the studies of tumor biopsies and well-characterized cell lines, the analysis of cancer biomarkers in blood can be utilized to aid disease diagnosis or prognostic goals [6, 7]. It is thus important to establish biochemical links between the glycosylated structures on the cell surfaces and those shed into the circulating biofluids.

Numerous studies on metastasis have mainly focused on genetic analysis using DNA microarrays or proteomic methodologies [8–12]. While highly informative in their own right, such studies are unable to identify glycans directly and discern their roles in metastasis. For example, poor prognosis of breast cancer correlates with increased quantities of mucins, a large protein family with extensive glycosylation. One of these proteins, mucin 1 (MUC1) is an approved Food and Drug Administration (FDA) biomarker for breast cancer through the use of a serum immunoassay test [13]. While MUC1 is a commonly used diagnostic indicator for detecting breast cancer, its overexpression does not necessarily correlate with distance metastasis [14].

In comparing cellular glycosylation of malignant and non-malignant cells and correlating such data with the glycosylated proteins in blood as the primary source of valuable diagnostic and prognostic information, it is essential to compare *structurally* and *quantitatively* the glycan profiles from relevant biological materials. Until recently, few bioanalytical methodologies were capable to perform such determinations. Through the recent advances in mass spectrometry (MS) of glycoconjugates [15, 16], the MS-based approaches are increasingly accepted as key methodologies in functional glycomics [17]. Recently, some preliminary data were shown for the glycans of human blood serum of ovarian, breast and prostate cancer patients and cell culture supernatant [7, 18–20] through the use of matrix-assisted laser desorption-ionization (MALDI) MS.

Our laboratory has recently developed and validated quantitative (solid-phase) permethylation [21], combined with MALDI-MS, as a powerful structural [22] and highly quantitative [6, 7, 20] methodology for glycomic profiling. In the present report, we demonstrate the use of this methodology in comparisons of the glycan profiles acquired from invasive and non-invasive breast cancer cells as well as normal breast epithelial cells used as a control. Quantitative glycan maps were derived form both N-linked and O-linked oligosaccharides, cleaved from both the cytosolic and membrane-bound glycoproteins, for comparative measurements among different cell types. Such comparisons are viewed here as the necessary prelude to a better understanding of the differences between cancerous and normal glycoproteomes, which, together with the data compiled on glycosyltransferases from DNA microarrays and extensive glycoproteomics investigations, could yield valuable insights into the nature of metastasis.

Results and discussion

General considerations

In performing comparative studies of glycosylation changes in different cancer cells, it was first essential to establish a quantitative and analytically reproducible method for profiling different classes of glycans. For the N- and O-linked oligosaccharides, this has primarily meant a reproducible cleavage [23, 24] from the extracted glycoproteins, followed by a mass-spectrometric display of different glycans. Quantitative permethylation at microscale levels [21] further ensures coverage of both neutral and sialylated oligosaccharide structures in a single analytical profile at adequate measurement sensitivity. The sensitivity enhancement through permethylation makes it not only practical to perform glycan profiling analyses with small amounts of cell lysate, but even more importantly, to compare these results

with the findings from small volumes of blood serum samples [6, 7] collected from cancer patients. Also, MALDI MS analyses of permethylated samples have been recently demonstrated to be highly quantitative [25]. Finally, a relatively high throughput of the overall analytical procedure has been important to perform comparative profiling on a statistically adequate number of samples.

While differential centrifugation has allowed us to make a distinction between the cytosolic proteins and membrane-associated proteins in the cell lysates of different samples, the enzymatic digestion with N-glycanase facilitated removal of N-glycans prior to β-elimination and a subsequent, separate analysis of O-linked oligosaccharides. The ability to analyze N-glycans and O-glycans mass-spectrometrically in separate fractions greatly simplifies data interpretation to a certain extent. While it had been expected and further verified in this work (see below) that the membrane-associated proteins overlap primarily with the glycans seen in the serum samples [6, 7] in being shed into the bloodstream, the information obtained from cytosolic proteins could still be valuable in judging a differential nature of subcellular trafficking phenomena in health and disease.

The different protein fractions were isolated from the cell lines, as described below, representing invasive breast cancer (MDA-MB-231 and MDA-MB-435), non-invasive breast cancer (578T, NCI/ADR-RES, BT549 and T47D) and normal epithelial breast cells (MCF10A). All cells were harvested during the log growth phase to ensure consistency.

Comparative analyses of N-glycans

Cytosolic proteins Representative glycomic profiles of N-glycans isolated from the cytosolic fraction of different cell types are depicted in Fig. 1, representing normal breast epithelial cells (a), invasive breast cancer cells (b) and non-invasive breast cancer cells (c). The structures of different N-glycans, as identified through tandem MS when possible, are labeled in the figures. The relative intensities of the individual N-glycans were calculated using an in-house developed computer tool, while the separate cell lines were examined in duplicate, with the exception of MCF10A, which was examined using four separate preparations. The data was further compiled and separated into arbitrary categories according to a structural type, with the exception of high-mannose structures being depicted individually (Fig. 2a).

As seen in Fig. 2, there seem to be some statistical differences in the overall composition of N-glycans derived from soluble cytosolic glycoproteins isolated from invasive and noninvasive relative to that isolated from normal epithelial cells. The majority of high-mannose structures (Fig. 2a) are statistically elevated in both invasive and non-invasive cancer cells when compared to the normal

Fig. 1 Representative MS profiles of permethylated N-glycans derived from cytosolic proteins in different cell lines: **a** MCF10A normal epithelial cells; **b** MDA-MB-435 invasive breast cancer cells; and **c** 578T non-invasive breast cancer cells
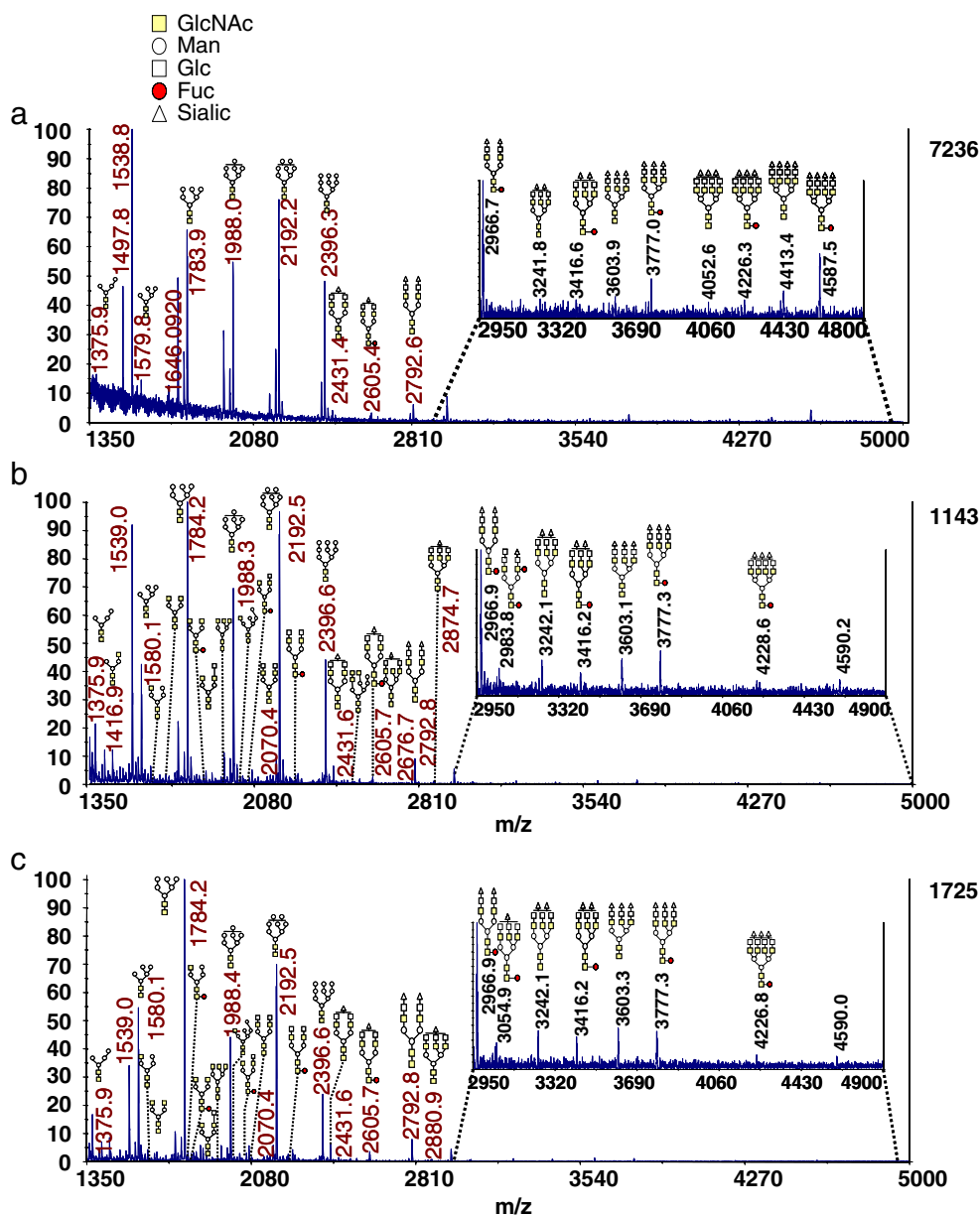
epithelial cells, except for $GlcNAc_2Man_4$ and $GlcNAc_2Man_9$ structures. The statistical significance is suggested by analysis of variance (ANOVA) testing represented as asterisks (Fig. 2). This evaluation was based on comparing the results of each of the cancer group to the normal cells. This is particularly evident for $GlcNAc_2Man_5$ and $GlcNAc_2Man_6$, which is consistent with the known increases of high-mannose structures in tumors [26, 27]. As our glycan profiling procedure also includes the hybrid and complex structures with multiantennary arrangements and a variable degree of fucosylation, we were also able to observe some trends (Fig. 2b) in these categories. In contrast to the high-mannose structures, the levels of other branching N-glycan types are generally lower in the cancer cells when compared to normal cells, and there is also a

significant decrease in the relative amounts of hybrid structures in both invasive and non-invasive cancer cells. The complex tetra-antennary structures and their fucosylated counterparts seem somewhat exceptional in this regard, although the overall intensities of mass-spectral peaks are relatively small in all cases, and thus implicating greater measurement errors. Again statistical evaluation of the data presented in Fig. 2b was based on ANOVA testing as reflected in the asterisks associated with each box graph.

We have also separated our data to reflect the overall level of sialylation and fucosylation (Fig. 2c). Given the level of increase seen in the high-mannose structures from both breast cancer cell types in relation to the normal epithelial cells, there is a significant decrease in both the sialylation and fucosylation in both cancer cell types. We
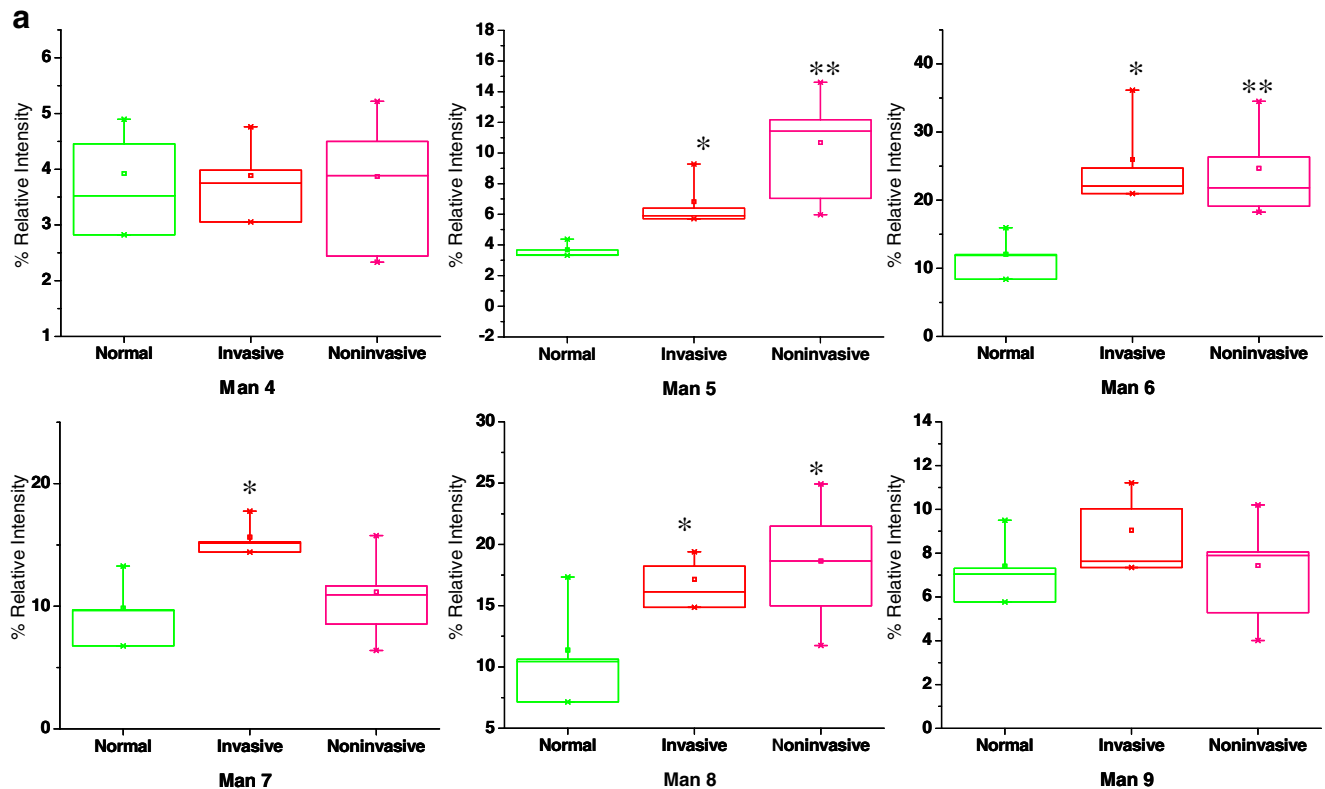
a

Fig. 2 Box graphs depicting the relative intensities of the N-glycans derived from cytosolic proteins of different cell types: **a** High-mannose oligosaccharides of different molecular mass; **b** Complex and hybrid structures (bi, tri- and tetra-antennary glycans, with or without fucosylation); and **c** Sialylated and fucosylated structures. Data were acquired from four preparations of normal cells, four preparations of invasive cells and eight preparations of noninvasive cells

observe a more pronounced loss of sialylation in the invasive cell type, but both cancer cell types are lower than normal cells. There is a slight, but noticeable decrease in the overall level of fucosylation in both cancer cell types, which was statistically confirmed through ANOVA testing. These data stand in contrast to the findings with the membrane-associated proteins (see below) and the levels in sera of cancer patients [6, 7].

Principal Component Analysis (PCA) of the acquired data was performed with all MS profiles to express analytical differences through a non-biased mechanism. The PCA step segregates the normal breast epithelial cells away from all breast cancer cells (Fig. 3). The normal breast cell recordings cluster together as opposed to the non-invasive breast cancer results, which vary substantially. This variance in non-invasive cells seems to be a reflection of real differences between the cells representing distinct phenotypic classifications.

Membrane-associated proteins Representative MS-based glycomic profiles for the N-glycans isolated from membrane-associated proteins are depicted for normal epithelial cells

(MCF10A) in Fig. 4a; for invasive breast cancer cells (MDA-MB-435) in Fig. 4b; and for non-invasive breast cancer cells (578T) in Fig. 4c. Similar to the comparison strategy used for the cytosolic proteins, described in the previous section, we plot the results obtained for different classes of glycans (Fig. 5) to point out potential differences in the glycosylation mechanisms.

Figure 5a represents the levels of individual high-mannose structures in all three types of cellular preparations. The levels appear mostly similar in both the invasive and non-invasive cancer cells, and comparable to normal epithelial cells. However, $GlcNAc_2Man_5$ increased in invasive cells and significantly increased in non-invasive cell samples. This increase roughly corresponded to a large decrease in $GlcNAc_2Man_9$ in the non-invasive cells when compared to the rest. The statistical significance of the differences observed in Fig. 5 were evaluated through ANOVA testing and it is presented as asterisks.

The remaining N-glycan structures were once again categorized by their branching features, just as described in "Cytosolic proteins", above. The complex tetra-antennary and tetra-antennary/fucosylated structures are increased in
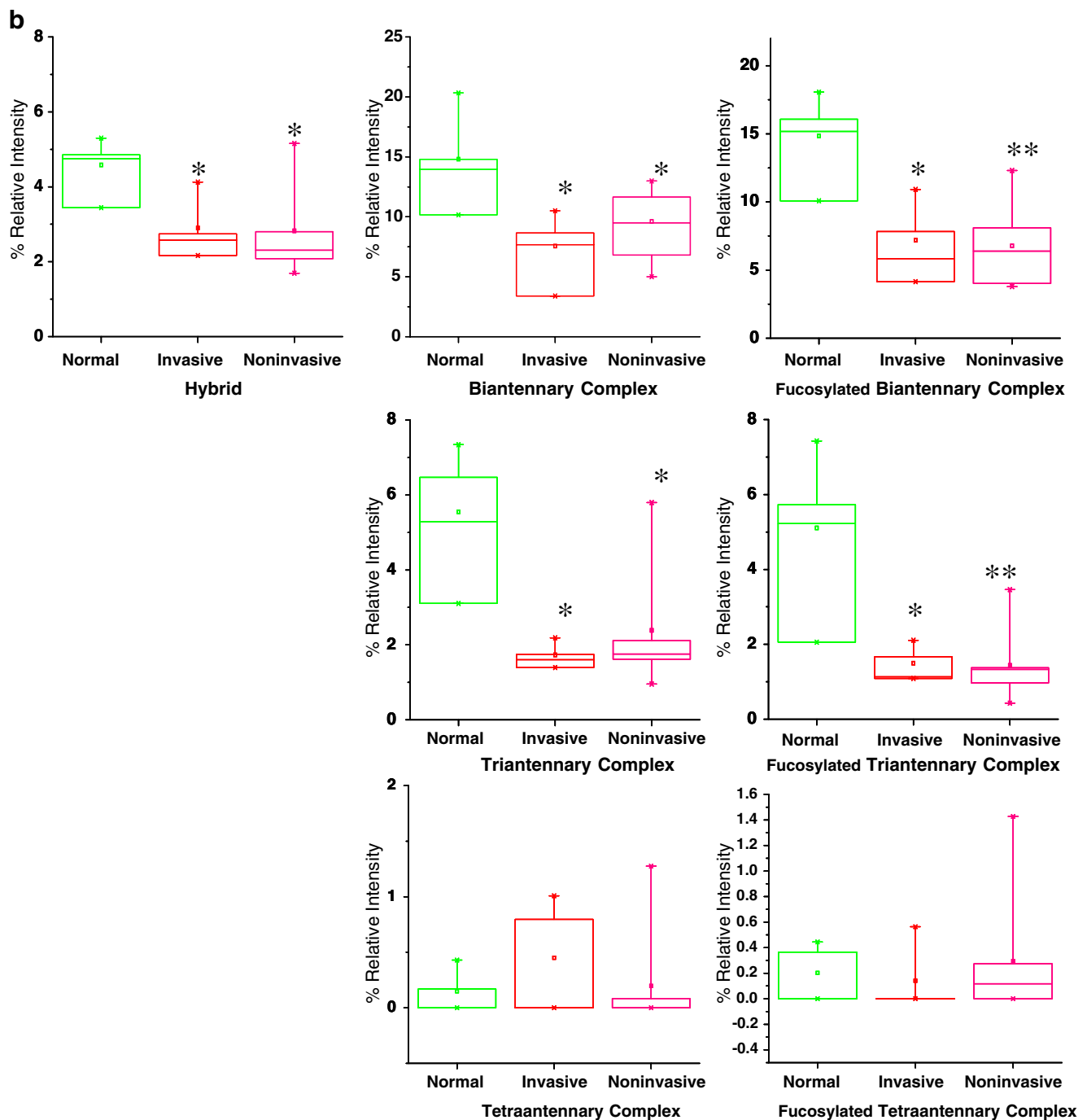
Fig. 2 (continued)

both the invasive and non-invasive cell types in comparison to the normal control; however, all the observed differences were not statistically significant. Unlike the N-glycans isolated from cytosolic proteins, there are no statistically significant differences in the di-antennary, tri-antennary and hybrid structures isolated from the membrane-associated glycoproteins when compared to control. The only difference

that was statistically significant was that of the tetraantennary complex structures derived from noninvasive cell lines

As in the previous analysis, the overall data were also separated into the groups reflecting the overall levels of sialylation and fucosylation in all structures. As seen in Fig. 5c, an increase in the overall degree of fucosylation for both the invasive and non-invasive cell lines is observed;
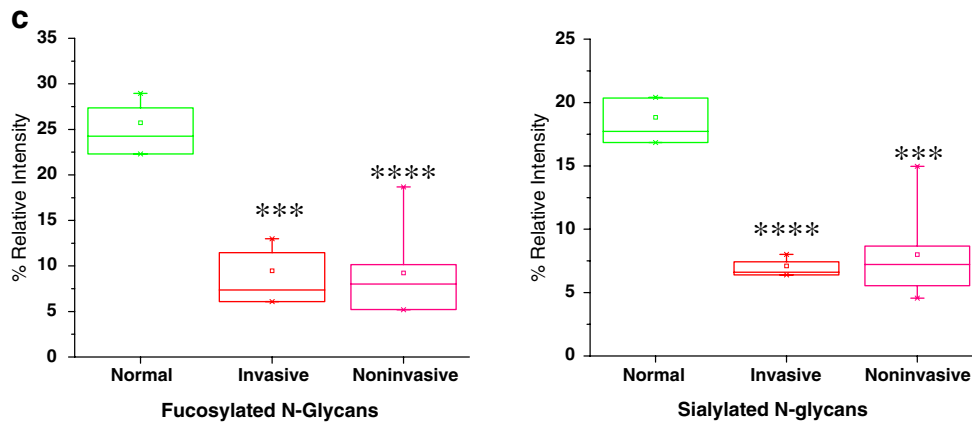
c

Fig. 2 (continued)

however, it is not statistically significant as suggested by ANOVA evaluation of the data. Also, there are no significant differences in the sialylation of glycans derived from cancer cell lines relative to the normal cell line.

The Principal Component Analysis was once again performed on the data extracted from all different cell lines for the membrane-associated protein fraction. The statistical evaluation procedure readily separated the normal epithelial

Fig. 3 PCA score graph of the N-glycan profile data derived from cytosolic proteins of different cell lines. The three *green circles* represent the normal epithelial cells, while the four *blue diamonds* belong to non-invasive cancer cells. The invasive cells are represented through *spotted circles*
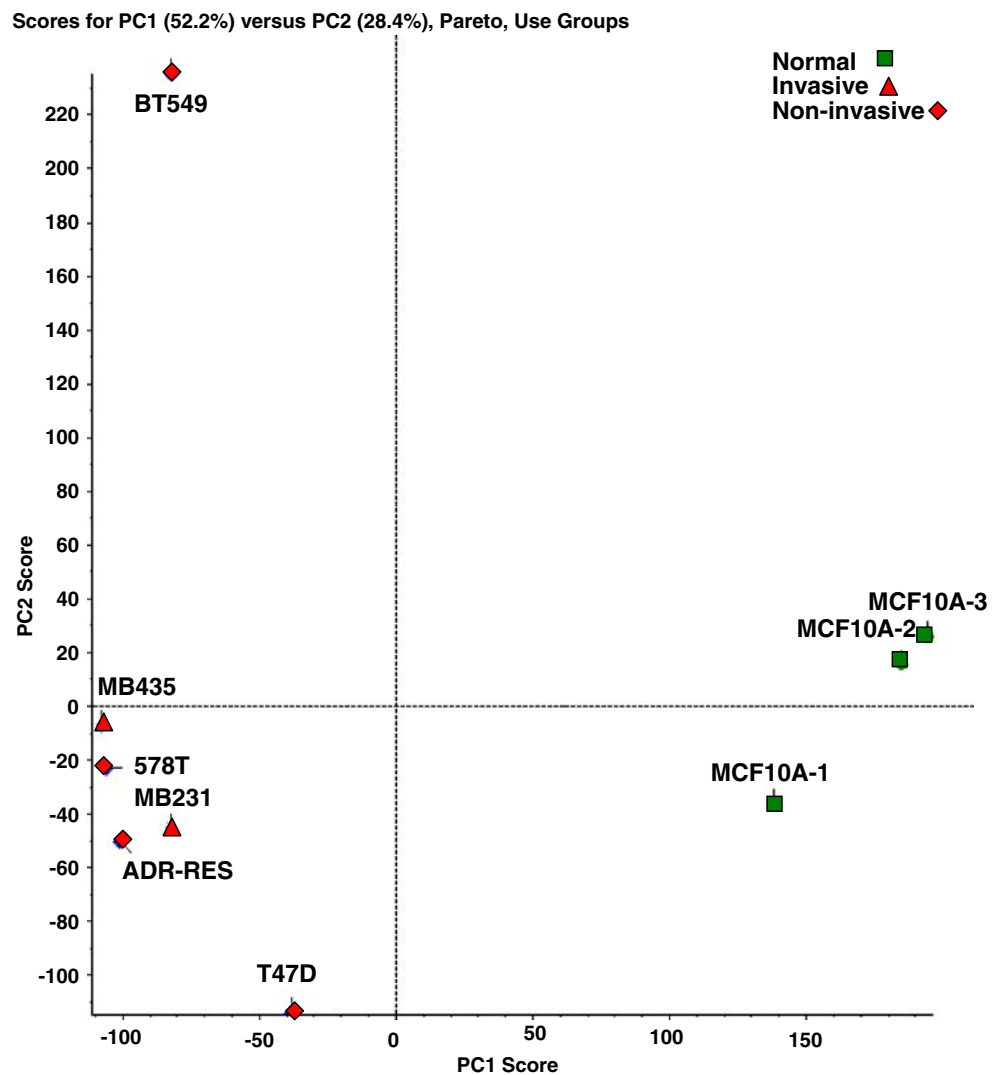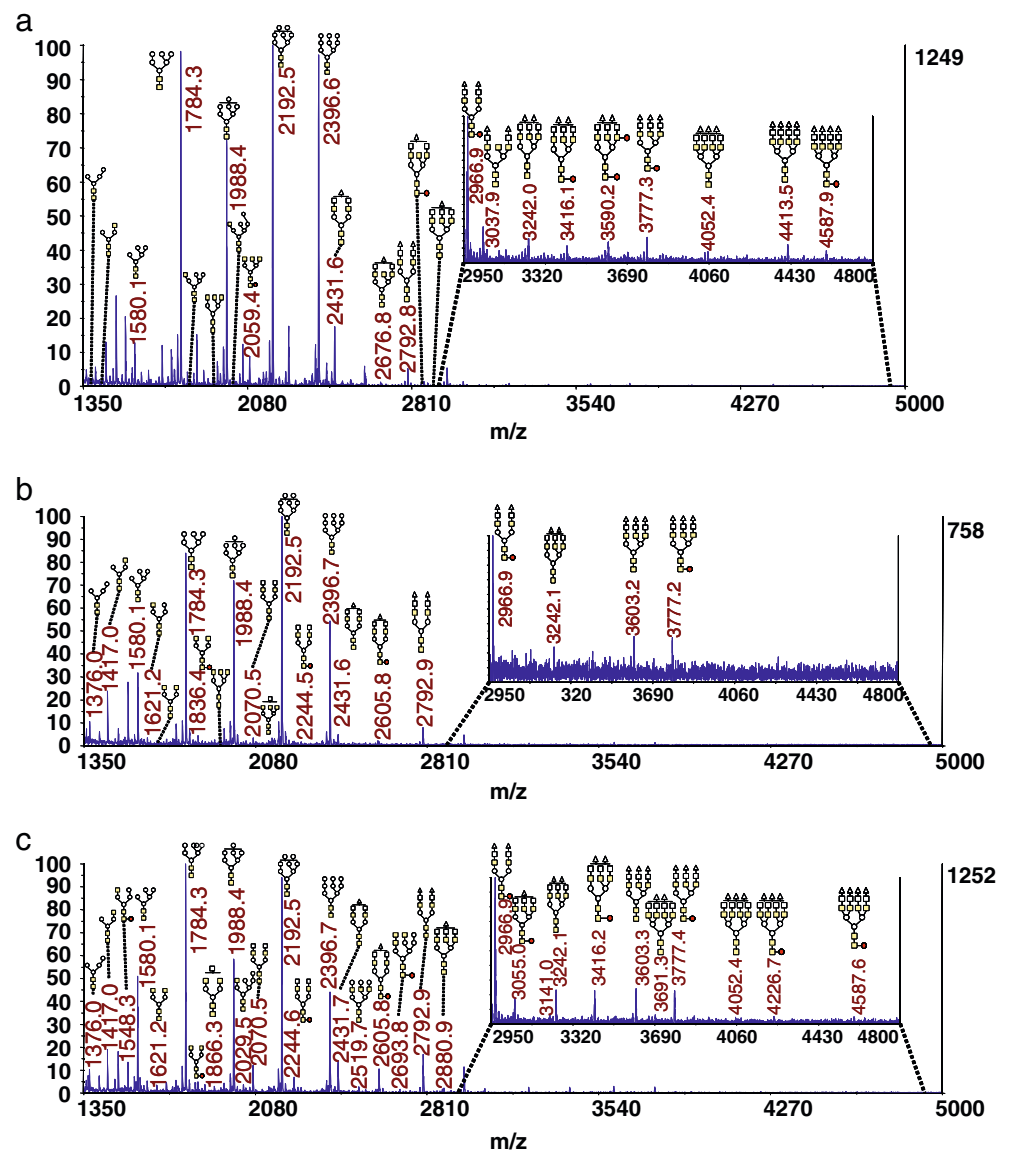
Fig. 4 Representative MS profiles of permethylated N-glycans derived from membrane-associated proteins in different cell lines. Designation of (**a**–**c**) is the same as in Fig. 1

and cancer cell lines into distinct clusters (data not shown), but failed to show any clear distinction between the invasive and non-invasive cells.

Comparative analyses of O-glycans

Unlike the N-linked glycans that represent more definitive structural assignments due to their well-defined consensus sequence, most O-linked structures profiled from the minute quantities of biological materials are currently tentative. In Fig. 6a–c, this is reflected by the sugar residue designations "Hex" for hexoses of thus far undefined structure, and "HexNAc" for their acetylated counterparts. Once again, this figure reflects representative O-linked oligosaccharide profiles comparing invasive and non-invasive cancer cells with normal breast epithelial cells.

After computing the relative O-glycan peak intensities, the compiled data were separated according to different structural types and compared (see Fig. 7 and Tables 1, 2, 3). The data analysis of the O-glycans isolated from cytosolic proteins indicate statistically significant changes in the overall level of fucosylation of invasive breast cancer cells compared to normal epithelial cells. The change in the non-invasive cells was not statistically significant although the overall level was increased.

It has been further instructive to separate our data in terms of the more detailed O-glycan structural types, as reflected in the remainder of Fig. 7. As seen, for example, in Table 1, there are numerous differences in the levels of different neutral O-glycans. Some of these structures were recently determined as important by another group [18, 19], through the use of different techniques. We see some
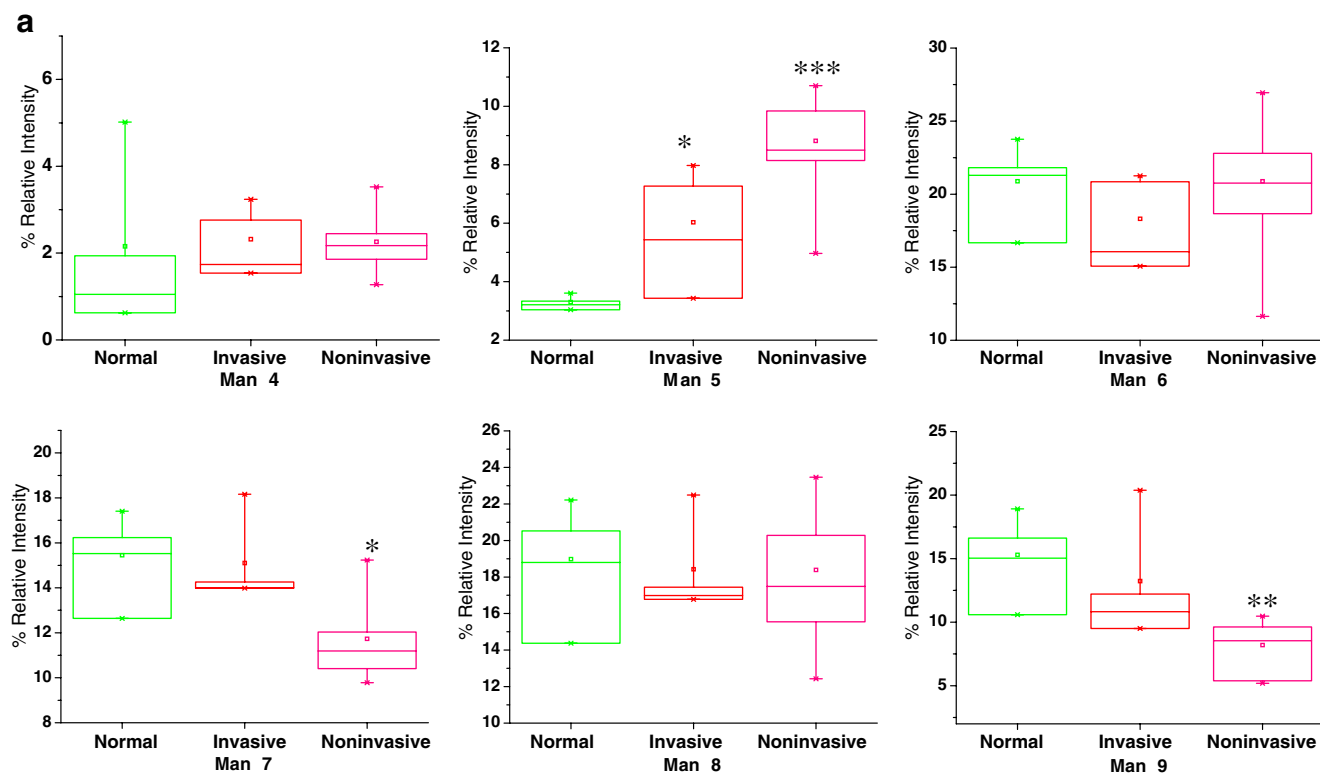
Fig. 5 Box graphs depicting the relative intensities of N-glycan derived form membrane-associated proteins in different cell lines. Designation of (**a**–**c**) is the same as in Fig. 2. Data were acquired from four preparations of normal cells, four preparations of invasive cells and eight preparations of noninvasive cells

differences that are consistent with their findings: for example, an increase in $HexNAc_2Hex_3$ and $HexNAc_2Hex_5$ is consistent; however, MS/MS analysis indicated the possibility that this m/z value might be attributed to both N- or O-glycans. These N-glycan structures are believed to originate from incomplete PNGase F digestion. The MS/MS spectra of these m/z values shaded in Table 1 and other tables (see below) contained distinct ion fragments originating from both N- and O-glycans, thus suggesting the presence of both fragments in the samples (data not shown).

When examining the fucosylated O-glycan structure, we obtain results which could potentially become useful indicators of a disease state (Table 2). While $HexNAc_2HexFuc$ is overwhelmingly expressed in normal epithelial cells, $HexNAc_2Hex_2Fuc$ and $HexNAc_2Hex_3Fuc$ are significantly enhanced in the invasive and non-invasive cells. These data suggest that the biosynthetic process for these oligosaccharides is being affected in the disease state in a very specific way.

The overall data were further partitioned to isolate the sialylated O-glycan structures. As seen in Table 3, there is a marked decrease amongst nearly all sialylated O-glycans isolated from both the invasive and non-invasive breast cancer cells. This observation indicates that there are some

defects in the sialylation pathway due to breast cancer, or significant increases in favor of fucosylation.

Through a non-biased mechanism of PCA, the spectral profiles of O-glycans were compared to discern any potential differences among the sample types. The PCA analysis has decidedly segregated the normal breast epithelial cells from the cancer cells (Fig. 8).

Moreover, the segregation was also achieved for the invasive and non-invasive cancer cells, representing potentially distinct phenotypic classifications. However, statistical analysis of the known structures did not reveal any significant differences between the O-glycans derived from invasive and non-invasive breast cancer cells, suggesting the differences to be due to the unresolved structures, which were not included in the statistical analysis.

Due to the high complexity of the O-glycan fractions isolated from membrane proteins, additional fractionation steps are currently being developed to provide more reliable quantification and characterization.

Conclusions

A comprehensive glycomic analysis of breast cancer cells performed in this study reveals potentially intriguing
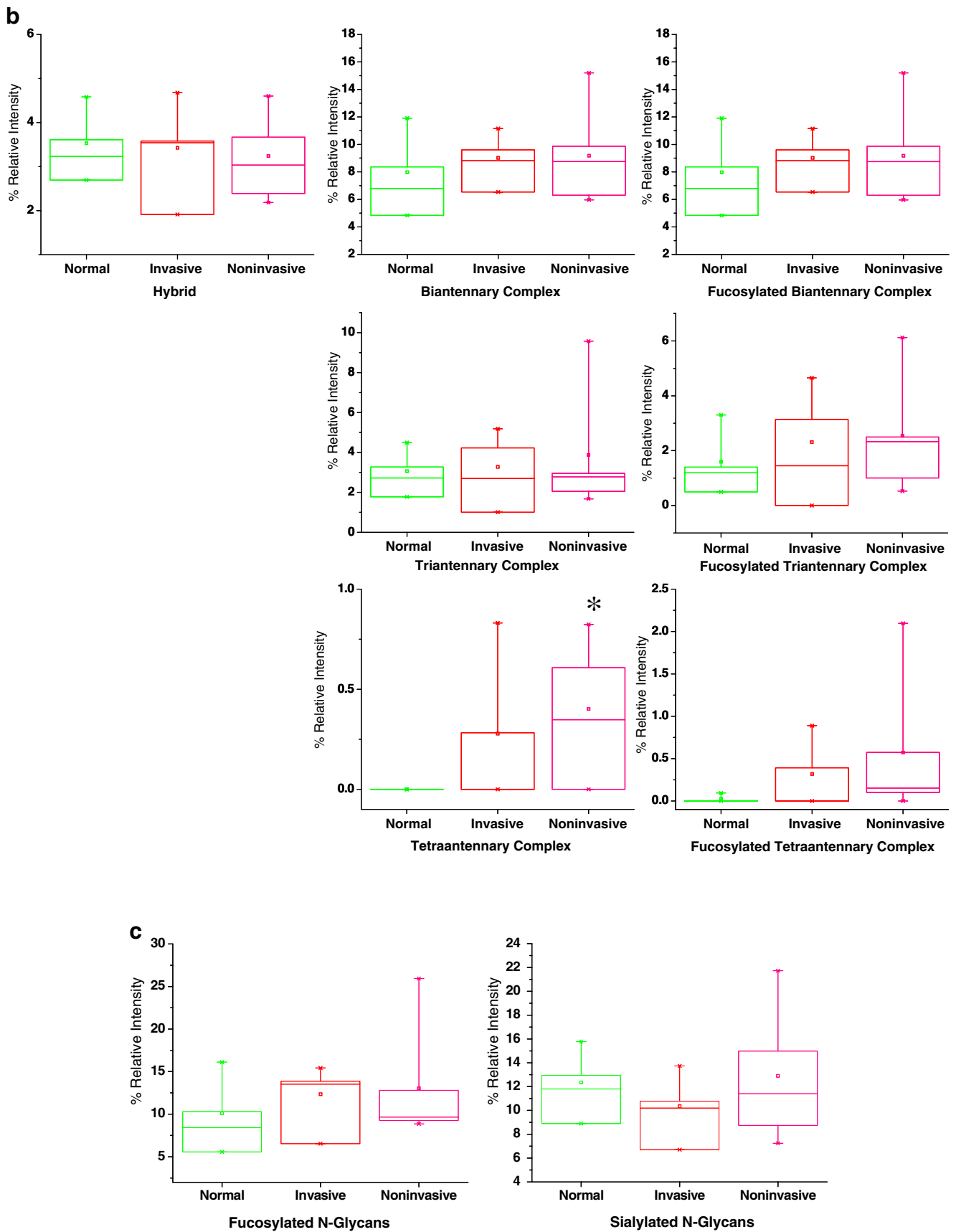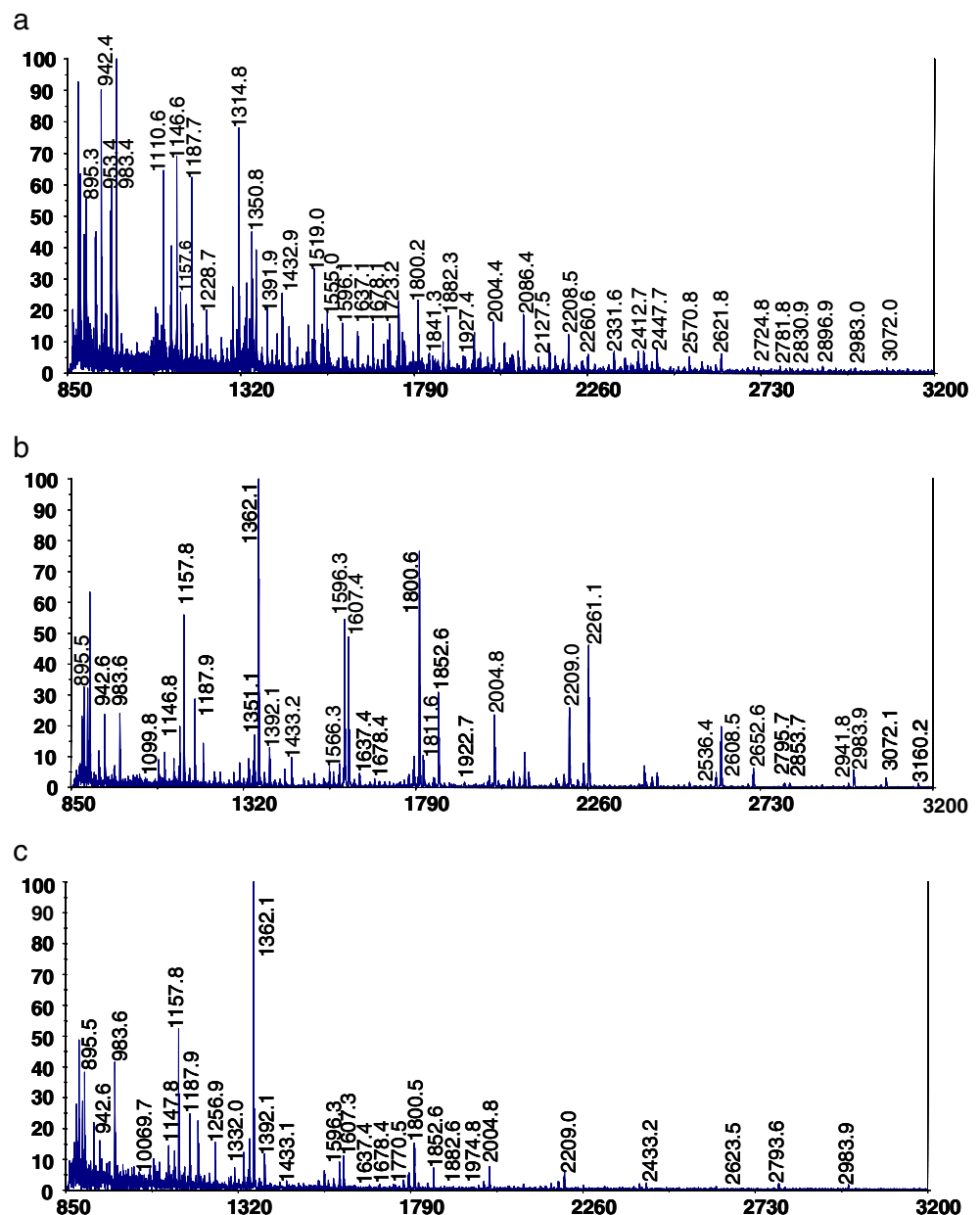
Fig. 5 (continued)

Fig. 6 Representative MS profiles of permethylated O-glycans derived from cytosolic proteins of different cell lines. Designation of (**a**–**c**) is the same as in Figs. 1 and 4

differences due to cancer and its invasive nature. Given the importance of metastasis in cancer mortality, these molecular insights could potentially be utilized therapeutically through prevention of specific steps in the glycosylation pathway. In identifying specific structures, one could target particular enzymes responsible for aberrant glycosylation, with the results similar to those in which precursors of sialyl Lewis X inhibit the metastasis of colon and lung cancer cells [28].

The obtained data can also be utilized in correlations with glycomic profiles obtained from the analyses of patient blood samples, illustrating importance of certain trends. In our recent work [6, 7, 20], differences in glycan intensities were noted for different breast cancer conditions. For example, one key observation made in that study was an enhancement in the

level of fucosylation of N-glycans, which increased progressively from the non-cancer condition to stage IV breast cancer through the lower stages of the disease. Correspondingly, we have seen increased fucosylation in O-glycans isolated from invasive cancer cells in this work. Thus, fucosylation of certain glycans could potentially be considered as a measure of cancer invasiveness and tumor progression.

In addition to the fucosylation changes, we have seen a significant decrease in sialylated structures for both N-glycans and O-glycans isolated from cytosolic proteins. This observation is not as evident in the membrane-associated proteins and also in serum samples [6, 7, 20]. However, this does not diminish its potential occurrence in solid tumors.
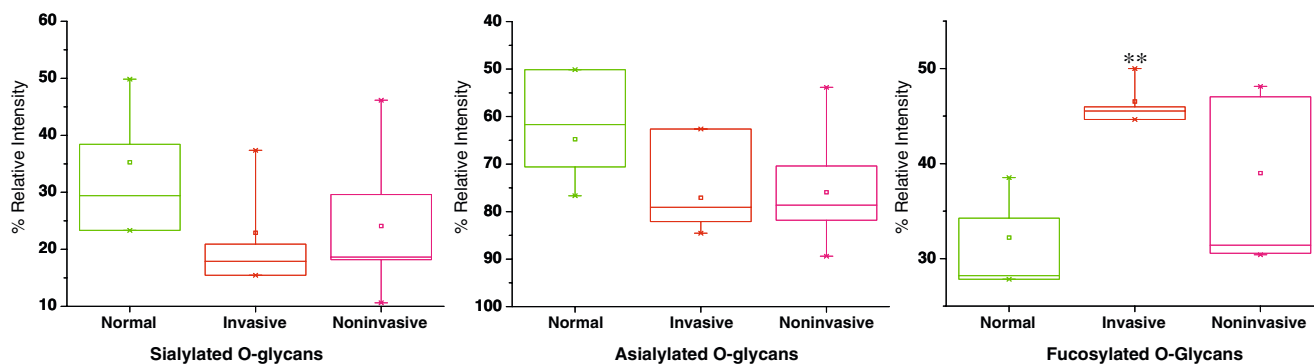
Fig. 7 Box graph depicting the relative intensities of non-sialylated, fucosylated, and sialylated O-glycans derived form cytosolic proteins of different cell lines. Data were acquired from four preparations of normal cells, four preparations of invasive cells and eight preparations of noninvasive cells

Given the earlier work of using inhibited glycosylation to slow metastasis and cell progression [29–31], it may not be so surprising to find significant differences in the glycomic profiles of invasive and non-invasive cancer cell lines. However, to this date, very little work has been done to assess a variety of seemingly related structures in a highly quantitative fashion. A more detailed continuation of these studies should undoubtedly be helpful to cancer research and diagnostic procedures.

Experimental section

Materials Sodium hydroxide (20–40 mesh beads) 97%, dimethyl sulfoxide (DMSO), 2,5-dihydroxybenzoic acid (DHB) and acetonitrile were acquired from Aldrich (Milwaukee, WI, USA). Chloroform was obtained from EM Science (Gibbstown, NJ, USA). Fused silica capillaries, 500 μm i.d.×750 μm o.d. were from Polymicro Technologies (Phoenix, AZ, USA), while PEEK tubing, 1 mm i.d., nuts and ferrules were purchased from Upchurch Scientific (Oak Harbor, WA, USA). Phenylmethylsulfonylfluoride (PMSF), iodomethane, sodium pyrophosphate, 3-[3-(cholamidopropyl)dimethylammonio]-1-propanesulfonate (CHAPS), Tris–HCl, ethylenediamine tetraacetic acid (EDTA), ethylene glycol bis(2-aminoethyl ether)tetraacetic acid (EGTA), borane–ammonia complex, dithiothreitol (DTT), and 28% aqueous ammonium hydroxide were acquired from Sigma Co. (St. Louis, MO, USA). PNGase F was purchased from Prozyme (San Leandro, CA, USA).

Breast cancer cell lines MDA-MB-435, MDA-MB-231, 578T, BT549, NCI/ADR-RES and T47D cell pellets were

Table 1 Relative intensities of non-sialylated/non-fucosylated O-glycans derived from cytosolic proteins of normal epithelial cells (MCF10A); invasive breast cancer cells (MDA-MB-435); and non-invasive breast cancer cells (578T)

Structure	Mass	Normal	Invasive	Non-invasive
$HexNAc_1Hex_3$	942.9	7.01±0.72	4.60±0.24	5.52±1.68
$HexNAc_2Hex_2$	983.8	9.08±0.48	9.47±0.44	5.91±0.69
$HexNAc_1Hex_4$	1,147.1	2.01±0.08	3.63±0.17	4.42±1.36
$HexNAc_2Hex_3$	1,188.0	3.56±0.42	5.63±0.29	5.77±0.37
$HexNAc_2Hex_4$	1,392.2	2.55±0.63	2.31±0.31	1.85±0.17
$HexNAc_3Hex_3$	1,433.1	1.01±0.12	0.61±0.04	0.66±0.11
$HexNAc_2Hex_5$	1,596.4	1.20±0.41	2.27±0.01	4.76±0.82
$HexNAc_3Hex_4$	1,637.3	0.57±0.07	0.53±0.06	0.56±0.10
$HexNAc_2Hex_6$	1,800.7	1.04±0.31	4.23±0.22	6.76±1.09
$HexNAc_3Hex_5$	1,841.6	1.23±0.30	0.21±0.01	0.30±0.07
$HexNAc_4Hex_4$	1,882.5	1.73±0.76	0.38±0.01	0.16±0.03
$HexNAc_2Hex_7$	2,004.9	0.92±0.07	1.68±0.01	1.75±0.41
$HexNAc_2Hex_8$	2,209.1	0.48±0.12	1.25±0.09	1.83±0.38
$HexNAc_2Hex_9$	2,413.3	0.04±0.03	0.60±0.17	0.57±0.05
$HexNAc_2Hex_{10}$	2,617.6	0.04±0.02	0	0
$HexNAc_2Hex_{11}$	2,821.8	0.07±0.04	0.09±0.04	0
$HexNAc_2Hex_{12}$	3,026.0	0.04±0.02	0	0

Shaded structures could be N- or O-linked glycans

Table 2 Relative intensities of fucosylated O-glycans derived from cytosolic proteins of normal epithelial cells (MCF10A); invasive breast cancer cells (MDA-MB-435); and non-invasive breast cancer cells (578T)

Structure	Mass	Normal	Invasive	Non-invasive
HexNAc$_2$HexFuc	953.6	9.08±0.96	1.81±0.06	0.59±0.02
HexNAc$_2$Hex$_2$Fuc	1,157.9	3.48±0.30	14.07±0.56	9.51±1.81
HexNAc$_2$Hex$_2$Fuc$_2$	1,332.0	1.85±0.13	0.79±0.02	0.31±0.02
HexNAc$_2$Hex$_3$Fuc	1,362.1	1.19±0.12	20.79±1.93	12.97±0.46
HexNAc$_4$HexFuc	1,443.9	1.44±0.13	0.32±0.00	0.10±0.01
HexNAc$_2$Hex$_2$Fuc$_3$	1,506.0	0.75±0.12	0.33±0.01	0.10±0.01
HexNAc$_3$Hex$_3$Fuc	1,607.2	0.56±0.05	2.70±0.04	4.33±0.94
HexNAc$_3$Hex$_3$Fuc$_2$	1,781.3	0.28±0.04	0.20±0.01	0.11±0.02
HexNAc$_4$Hex$_3$Fuc	1,852.3	0.30±0.11	1.57±0.08	2.36±0.56
HexNAc$_4$Hex$_3$Fuc$_3$	1,955.4	0.15±0.04	0.10±0.05	0.13±0.02
HexNAc$_4$Hex$_3$Fuc$_2$	2,026.4	0.12±0.04	0.12±0.06	0.06±0.02
HexNAc$_4$Hex$_4$Fuc	2,056.6	0.91±0.42	0.29±0.02	0.43±0.09
HexNAc$_4$Hex$_4$Fuc$_2$	2,230.7	0.27±0.06	0.09±0.05	0.17±0.05
HexNAc$_4$Hex$_5$Fuc	2,260.8	0.99±0.50	0.99±0.29	2.72±0.77
HexNAc$_4$Hex$_4$Fuc$_3$	2,404.7	0.19±0.02	0.08±0.04	0.07±0.01
HexNAc$_4$Hex$_4$Fuc$_4$	2,578.8	0.06±0.04	0	0.03±0.01

Shaded structures could be N- or O-linked glycans

obtained through the Developmental Therapeutics Program (DTP) of the National Cancer Institute (http://dtp.nci.nih. gov/). The control normal breast epithelial cell line (MCF10A) was cultured as previously described [32]. Cell pellets were prepared as described by the DTP [33].

Cell lysis and sample preparation Cell pellets were prepared from 150 mm tissue culture plates, and on average 1×10^7 cells were used per experiment. Cells were lysed using 400 μl of a CHAPS-based buffer consisting of 150 mM NaCl, 0.5% CHAPS, 20 mM Tris–HCl (pH 7.5),

Table 3 Relative intensities of sialylated O-glycans derived from cytosolic proteins of normal epithelial cells (MCF10A); invasive breast cancer cells (MDA-MB-435); and non-invasive breast cancer cells (578T)

Structure	Mass	Normal	Invasive	Non-invasive
HexNAcHexNeuNAc	895.6	8.47±1.16	8.22±0.46	20.04±5.41
HexNAc$_2$NeuNAc	936.5	9.06±1.93	1.53±0.09	0.39±0.03
HexNAcHexFucNeuNAc	1,069.7	8.24±0.86	1.26±0.11	0.26±0.01
HexNAcHex$_2$NeuNAc	1,099.8	6.74±0.75	2.19±0.27	0.80±0.07
HexNAc$_2$HexNeuNAc	1,140.7	4.80±0.53	0.84±0.12	0.43±0.05
HexNAc$_2$Hex$_2$NeuNAc	1,344.9	1.24±0.12	0.94±0.19	0.63±0.08
HexNAc$_2$Hex$_2$FucNeuNAc	1,519.0	0.90±0.14	0.46±0.02	0.09±0.02
HexNAc$_3$HexFucNeuNAc	1,559.9	0.63±0.04	0.26±0.00	0.11±0.01
HexNAc$_3$Hex$_2$NeuNAc	1,590.1	0.53±0.08	0.19±0.01	0.04±0.01
HexNAc$_2$Hex$_3$FucNeuNAc	1,723.3	0.42±0.13	0.12±0.06	0.05±0.02
HexNAc$_3$Hex$_2$FucNeuNAc	1,764.2	0.45±0.09	0.27±0.04	0.09±0.01
HexNAc$_3$Hex$_3$NeuNAc	1,794.3	0.27±0.08	0.12±0.06	0.11±0.02
HexNAc$_3$Hex$_3$FucNeuNAc	1,968.4	0.20±0.03	0.18±0.01	0.09±0.02
HexNAc$_3$Hex$_4$NeuNAc	1,998.5	0.29±0.04	0.24±0.03	0.15±0.04
HexNAc$_3$Hex$_3$Fuc$_1$NeuNAc	2,142.5	0.07±0.04	0.11±0.06	0.08±0.01
HexNAc$_3$Hex$_5$NeuNAc	2,202.7	0.11±0.03	0	0.11±0.03
HexNAc$_3$Hex$_3$Fuc$_3$NeuNAc	2,316.6	0.24±0.10	0.11±0.06	0.04±0.01
HexNAc$_4$Hex$_4$FucNeuNAc	2,417.7	0.31±0.04	0.21±0.01	0.18±0.03
HexNAc$_4$Hex$_4$Fuc$_2$NeuNAc	2,591.8	0.17±0.05	0.09±0.05	0.02±0.01
HexNAc$_4$Hex$_4$NeuNAc$_2$	2,604.8	0.09±0.03	0.07±0.04	0.01±0.01
HexNAc$_4$Hex$_5$FucNeuNAc	2,622.0	0.19±0.06	0.57±0.19	1.24±0.27

Shaded structures could be N- or O-linked glycans

Fig. 8 PCA score graph of the O-glycan profile data derived from cytosolic proteins of different cell lines. The three *green squares* represent the normal epithelial cells, while three *red diamonds* belong to non-invasive cancer cells. The invasive cells are represented with *red triangle*
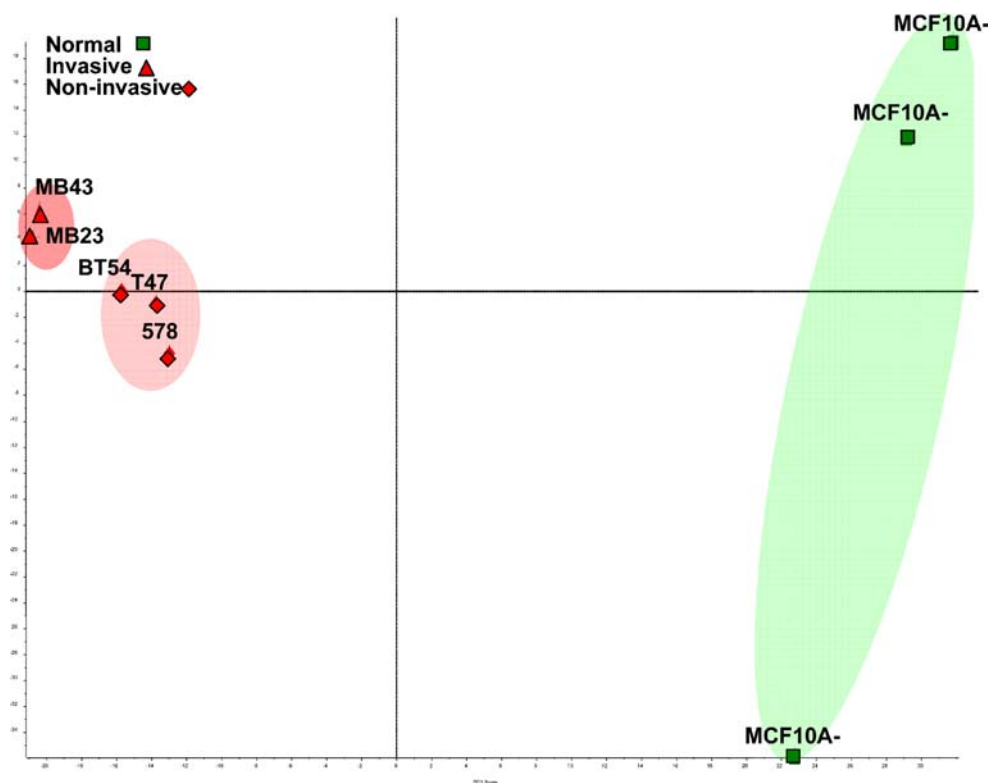
2.5 mM sodium pyrophosphate, with 1 mM EDTA and 1 mM EGTA. Cells were incubated in the lysis buffer at 4°C for 1 h and then centrifuged at $100,000 \times g$ for 90 min. The supernatant containing cytosol proteins was removed after centrifugation and the resulting pellet was resolubilized in CHAPS buffer and sonicated. The pellet contains membrane-associated proteins. The cytosolic proteins were then quantified using the Bradford assay [34]. Both cytosolic and membrane proteins were reduced and alkylated using 10 mM DTT at 56°C for 45 min and 55 mM iodoacetamide for 30 min, respectively, in the dark at room temperature. The reduced and alkylated proteins were then enzymatically digested using proteomics grade trypsin at 37°C overnight.

Release of N-glycans After tryptic digestion, samples were heated to 95°C for 10 min to deactivate trypsin. PMSF was then added to the samples at 0.5 mM concentration to ensure inhibition of trypsin. Sodium phosphate buffer (10 mM) was then added to the samples along with 2-mercaptoethanol for a final concentration of 0.1%. PNGase F was then added to the samples, which were incubated overnight at 37°C.

Solid-phase extraction and purification of released N-glycans The released N-glycans were extracted and purified using C18 and activated charcoal solid-phase extraction cartridges. Sep-Pak Classic C18 cartridges (Waters, Milford, MA, USA) were washed and equilibrated with ethanol and water, respectively. All samples were diluted up to 1 ml with water and passed over the cartridge five times. Cartridges were

then washed with a 1-ml aliquot of water. The resulting eluents containing the liberated N-glycans were then subjected to a solid-phase extraction using MicroSpin charcoal columns (Harvard Apparatus, Hamden, CT, USA). The peptides and O-linked peptides retained on the C18 cartridges were then eluted using 85% acetonitrile/H_2O (*v/v*) solution containing 0.1% trifluoroacetic acid. The C18 cartridge eluents were evaporated overnight using an Eppendorf Vacufuge.

N-glycans released by the PNGase F digestion and isolated through C18 cartridges were purified using Micro-Spin charcoal columns. Columns were washed and activated according to the manufacturer's protocol. Samples in aqueous solution were then applied and washed first using H_2O and then 5% acetonitrile/H_2O (*v/v*) solution containing 0.1% trifluoroacetic acid. Salts and other by-products were eluted during the washing step, while the N-glycans retained on the activated charcoal microspin columns were recovered using a 0.25-ml aliquot of 50% acetonitrile/H_2O (*v/v*) containing 0.1% trifluoroacetic acid. This wash was repeated four times and all eluents were collected and evaporated using an Eppendorf Vacufuge.

β-Elimination for O-glycan release Peptides eluted from the C18 cartridges were subjected to β-elimination to release O-glycans. Borane–ammonia complex solution was prepared by dissolving 5 mg/ml of borane–ammonia complex in 28% aqueous ammonia solution. A 15-μl aliquot of this solution was added to each of the samples. The reaction was then allowed to proceed at 45°C for 18 h.

The ammonia was then thoroughly removed from the samples using an Eppendorf Vacufuge. The samples were then reconstituted using 40 μl water and passed over a column made from a hydrophobic resin (Supelco SP20SS) and a strongly acidic cation exchange resin (Dowex 50 W× 8–400) [23, 24]. The sample was recirculated over the column five times, and the column was finally washed with 200 μl water. All eluents were collected and dried using Eppendorf Vacufuge.

Solid-phase permethylation of glycans Both the liberated N-glycans and O-glycans were then subjected to solid-phase permethylation. Samples were first reconstituted in a mixture of 69.2% DMSO, 30.4% iodomethane and 0.4% H_2O. Samples were then passed over a capillary column packed with sodium hydroxide as previously described [21]. After permethylation, samples were then extracted using chloroform and water to eliminate DMSO. Permethylated glycans retained in the chloroform layer were then dried using an Eppendorf Vacufuge.

MALDI analysis of oligosaccharides Mass spectra were recorded using an Applied Biosystems (Framingham, MA, USA) 4800 Proteome Analyzer (time-of-flight/time-of-flight mass spectrometer). DHB was used as the matrix (10 mg/ml in H_2O) in the positive ion mode. The permethylated oligosaccharides were resuspended in 5 μl of 50% methanol aqueous solution containing 1 mM sodium acetate. A 0.5-μl aliquot of the resuspended sample was then spotted on the MALDI plate and mixed with the matrix at a 1:1 ratio. Samples were then dried under vacuum before MALDI-MS analysis. MS measurements in the case of permethylated glycans were performed over 850–3,200 range. Although it is known that some O-glycans have m/z values smaller than 850, matrix clusters dominate MALDI mass spectrum below the range used in this study.

Relative intensity determination of mass spectra For calculating the relative intensities of the N-glycans or O-glycans in a profile, we utilized the PeakCalc program which was developed in-house. The PeakCalc program looks for a user-edited list of masses corresponding to the masses of either N- or O-glycans. The data extracted through this program were then verified manually, while the relative intensities of the different glycans were then calculated.

PCA analysis of mass-spectral data PCA [35] of N-glycans or O-glycans was performed using a MarkerView software (Applied Biosystems).

References

1. Tang, D.G., Honn, K.V.: Adhesion molecules and tumor metastasis: an update. Invasion Metastasis **14**(1–6), 109–122 (1994)
2. Kannagi, R.: Carbohydrate-mediated cell adhesion involved in hematogenous metastasis of cancer. Glycoconj. J. **14**(5), 577–584 (1997)
3. Fukuda, M.: Possible roles of tumor-associated carbohydrate antigens. Cancer Res. **56**(10), 2237–2244 (1996)
4. Kansas, G.S.: Selectins and their ligands: current concepts and controversies. Blood **88**(9), 3259–3287 (1996)
5. Leong, S.P., et al.: Clinical patterns of metastasis. Cancer Metastasis Rev. **25**(2), 221–232 (2006)
6. Kang, P., et al.: Comparative glycomic mapping through quantitative permethylation and stable-isotope labeling. Anal. Chem. **79**(16), 6064–6073 (2007)
7. Kyselova, Z., et al.: Breast cancer diagnosis and prognosis through quantitative measurements of serum glycan profiles. Clin. Chem. **54**, 1166–1175 (2008)
8. Hathout, Y., et al.: Proteomic phenotyping: metastatic and invasive breast cancer. Cancer Lett. **210**(2), 245–253 (2004)
9. Jiang, D., et al.: Identification of metastasis-associated proteins by proteomic analysis and functional exploration of interleukin-18 in metastasis. Proteomics **3**(5), 724–737 (2003)
10. Kluger, H.M., et al.: cDNA microarray analysis of invasive and tumorigenic phenotypes in a breast cancer model. Lab. Invest. **84**(3), 320–331 (2004)
11. Nishizuka, I., et al.: Analysis of gene expression involved in brain metastasis from breast cancer using cDNA microarray. Breast Cancer **9**(1), 26–32 (2002)
12. Tanaka, H., et al.: Differential gene expression screening between parental and highly metastatic pancreatic cancer variants using a DNA microarray. J. Exp. Clin. Cancer. Res. **22**(2), 307–313 (2003)
13. Bjerner, J., et al.: MUC1 serum assays in breast cancer: tumor specificities and reference levels. Tumour Biol. **23**(6), 315–323 (2002)
14. Rakha, E.A., et al.: Expression of mucins (MUC1, MUC2, MUC3, MUC4, MUC5AC and MUC6) and their prognostic significance in human breast cancer. Mod. Pathol. **18**(10), 1295–1304 (2005)
15. Miyamoto, S.: Clinical applications of glycomic approaches for the detection of cancer and other diseases. Curr. Opin. Mol. Ther. **8**(6), 507–513 (2006)
16. Novotny, M.V., Mechref, Y.: New hyphenated methodologies in high-sensitivity glycoprotein analysis. J. Sep. Sci. **28**(15), 1956–1968 (2005)
17. Raman, R., et al.: Glycomics: an integrated systems approach to structure–function relationships of glycans. Nat. Methods **2**(11), 817–824 (2005)
18. An, H.J., et al.: Profiling of glycans in serum for the discovery of potential biomarkers for ovarian cancer. J. Proteome Res. **5**(7), 1626–1635 (2006)
19. Kirmiz, C., et al.: A serum glycomics approach to breast cancer biomarkers. Mol. Cell Proteomics **6**, 43–55 (2007)
20. Kyselova, Z., et al.: Alterations in the serum glycome due to metastatic prostate cancer. J. Proteome Res. **6**, 1822–1832 (2007)

21. Kang, P., *et al*.: Solid-phase permethylation of glycans for mass spectrometric analysis. Rapid Commun. Mass Spectrom. **19**(23), 3421–3428 (2005)

22. Mechref, Y., Kang, P., Novotny, M.V.: Differentiating structural isomers of sialylated glycans by matrix-assisted laser desorption/ionization time-of-flight/time-of-flight tandem mass spectrometry. Rapid Commun. Mass Spectrom. **20**(8), 1381–1389 (2006)

23. Huang, Y., *et al*.: Matrix-assisted laser desorption/ionization mass spectrometry compatible beta-elimination of O-linked oligosaccharides. Rapid Commun. Mass Spectrom. **16**(12), 1199–1204 (2002)

24. Huang, Y., Mechref, Y., Novotny, M.V.: Microscale nonreductive release of O-linked glycans for subsequent analysis through MALDI mass spectrometry and capillary electrophoresis. Anal. Chem. **73**(24), 6063–6069 (2001)

25. Wada, Y., Azadi, P., Costello, C., Dell, E.A., Dwek, R.A., Geyer, H., *et al*.: Glycobiology **17**, 411–422 (2007)

26. Kui Wong, N., *et al*.: Characterization of the oligosaccharides associated with the human ovarian tumor marker CA125. J. Biol. Chem. **278**(31), 28619–28634 (2003)

27. Nuck, R., *et al*.: Comparative study of high-mannose-type oligosaccharides in membrane glycoproteins of rat hepatocytes and different rat hepatoma cell lines. Eur. J. Biochem. **216**(1), 215–221 (1993)

28. Asada, M., *et al*.: Increased expression of highly branched N-glycans at cell surface is correlated with the malignant phenotypes of mouse tumor cells. Cancer Res. **57**(6), 1073–1080 (1997)

29. Fuster, M.M., *et al*.: A disaccharide precursor of sialyl Lewis X inhibits metastatic potential of tumor cells. Cancer Res. **63**(11), 2775–2781 (2003)

30. Alper, J.: Glycobiology. Turning sweet on cancer. Science **301** (5630), 159–160 (2003)

31. Brown, J.R., *et al*.: A disaccharide-based inhibitor of glycosylation attenuates metastatic tumor cell dissemination. Clin. Cancer Res. **12** (9), 2894–2901 (2006)

32. Soule, H.D., *et al*.: Isolation and characterization of a spontaneously immortalized human breast epithelial cell line, MCF-10. Cancer Res. **50**(18), 6075–6086 (1990)

33. Nishizuka, S., *et al*.: Proteomic profiling of the NCI-60 cancer cell lines using new high-density reverse-phase lysate microarrays. Proc. Natl. Acad. Sci. U. S. A. **100**(24), 14229–14234 (2003)

34. Bradford, M.M.: A rapid and sensitive method for the quantitation of microgram quantities of protein utilizing the principle of protein-dye binding. Anal. Biochem. **72**, 248–254 (1976)

35. Verhoeckx, K.C., *et al*.: A combination of proteomics, principal component analysis and transcriptomics is a powerful tool for the identification of biomarkers for macrophage maturation in the U937 cell line. Proteomics **4**(4), 1014–1028 (2004)